JOURNAL OF KUFA–PHYSICS
journal.uokufa.edu.iq/index.php/jkp/index | ISSN: 2077–5830

The spectral properties and dispersion parameters of electrospun nanofibers (Poly vinyl alcohol/ Poly acrylamide)

Maher Hassan Rasheed **Hashim F.S** **Khalid Haneen Abass**

Department of Physics, College of Education for Pure Sciences, University of Babylon, Hilla, Iraq

Corresponding Author E-mail: bsc.maher.hassan@uobabylon.edu.iq

ARTICLE INF

Article history:
Received: 23 MAY., 2023
Revised: 23 JUN., 2023
Accepted: 05 JUL., 2023
Available Online: 18 DEC., 2023

Keywords:

Electrospun nanofibers, Spectral properties, Dispersion parameters.

ABSTRACT

Electrospun nanofibers based on polyvinyl alcohol (PVA), polyacrylamide (PAAm), and a PVA-PAAm blend (50/50 wt.%) were effectively made a room temperature(RT) and a voltage of (12kV).The products were studied using Field Emission Scanning Electron Microscope (FESEM), X-ray diffraction (XRD),Fourier-transform infrared spectroscopy(FT-IR) and Ultraviolet visible (UV–Vis) spectroscopy. The result of FESEM analysis showed that the polymer PVA, PAAm, and blend samples produced a random distribution of fine fibers at an average diameter of (214.12, 317.1, 157.65) nm with a smooth surface. In addition, the FESEM images demonstrate the fibres' suitability for use in gas sensing applications due to their branching fibres and porosity surface. XRD showed that the film polymeric of PVA, PAAm polymeric blend PVA-PAAm was seen to have a semicrystalline nature. According to the FTIR analysis, the PVA and PAAm networks in the PVA-PAAm polymer nanofibers were entangled due to the powerful hydrogen bond contact between the PAAm and PVA chains. Observed around (3473.79 and 3414) cm^{-1} were attributed to the N–H the vibration and overlapped to O–H stretching. The spectra of the prepared films exhibit prominent absorption peaks, which are at the wavelength range (200-320) nm. PVA-PAAm polymer nanofibers decrease the energy gap from 3.70eV to 3.40eV. The Wemple-DiDomenico model was used to derive dispersion parameters such as dispersion energy(E_d), single oscillator energy(E_0), Urbach energy (E_U),the static refractive index (n_0) and the moments of optical spectra($M_{-1}$and M_{-3}) the result of calculating (E_g) by this model was compatible with that value calculated by the Tauc relation. While$(E_d), (E_U), (n_0) and (M_{-1}\ M_{-3})$ increased which qualifies them to be used in the electronic devices.

DOI: https://doi.org/10.31257/2018/JKP/2023/v15.i02.12776

الخصائص الطيفية ومعلمات التشتت للألياف النانوية المحلولة كهربائيًا (البولي فينيل الكحول / البولي أكريلاميد)

ماهر حسن رشيد فؤاد شاكر هاشم خالد حنين عباس

[1]قسم الفيزياء ,كلية التربية للعلوم الصرفة ,جامعة بابل

الـــخُـــلاصـــة

تم تحضير ألياف نانوية مستندة إلى كحول البولي فينيل (*PVA*)، بولي أكريلاميد (*PAAm*)، ومزيج *PVA-PAAm* (بنسبة 50/50 وزنيًا) بفعالية عند درجة حرارة الغرفة (*RT*) وجهد (12 كيلو فولت). تم دراسة المنتجات باستخدام مجهر المجال الإلكتروني بالانبعاثات الحقلية (*FESEM*)، وتفاضل الأشعة السينية (*XRD*)، وطيف الأشعة تحت الحمراء بالتحويل الفوريه (*FT-IR*)، وطيف الأشعة فوق البنفسجية المرئية (*UV-Vis*). أظهرت نتائج تحليل *FESEM* أن عينات البوليمر *PVA*، *PAAm*، والمزيج تنتج توزيعًا عشوائيًا لألياف دقيقة بقطر متوسط (214.12، 317.1، 157.65) نانومتر بسطح ناعم. بالإضافة إلى ذلك، تظهر صور *FESEM* ملائمة الألياف للاستخدام في تطبيقات الكشف عن الغاز بسبب فروعها وسطحها المسامي. أظهرت *XRD* أن الأفلام البوليمرية لـ *PVA*، *PAAm*، ومزيج *PVA-PAAm* كانت تمتلك طبيعة شبه بلورية. ووفقًا لتحليل *FTIR*، تم تشابك شبكات *PVA* و *PAAm* في ألياف البوليمر *PVA-PAAm* نتيجة للروابط الهيدروجينية القوية بين سلاسل *PAAm* و *PVA*. تم ربط الترددات الملاحظة حول (3473.79 و 3414) سم-1 بالاهتزاز *N–H* والتمدد *O–H*. تكشف طيفية الأفلام المحضرة عن ذروة امتصاص بارزة في نطاق الطول الموجي (200-320) نانومتر. تقلل ألياف البوليمر *PVA-PAAm* النانوية الفجوة الطاقوية من 3.70 إلى 3.40 إلكترون فولت. تم استخدام نموذج *Wemple-DiDomenico* لاستنتاج معلمات التشتت مثل طاقة التشتت (E_d)، وطاقة المذبذب الفردية (E_0)، وطاقة *Urbach* (E_U)، ومعامل الانكسار الساكن (n_0) ولحظات الطيف البصري (M_{-1})و(M_{-3}). أظهرت النتيجة لحساب (E_g) بواسطة هذا النموذج توافقها مع القيمة المحسوبة بواسطة علاقة *Tauc*. بينما زادت(E_u),(E_d)، (n_0) ، و (M_{-1})(M_{-3}) مما يؤهلها للاستخدام في الأجهزة الإلكترونية.

الكلمات المفتاحية:

الألياف النانوية الملتفة كهربائيا، الخصائص الطيفية، معاملات التشتت

1. Introduction

Polymers have quickly become an essential component of contemporary life.This is because of their versatility and low cost, low operating costs, simple processability, and desirable chemical, physical, and optical qualities [1,2]: Each molecule in a polymer is made up of thousands of atoms held together by covalent chemical bonds, and the molecules in a polymer are attracted to one another by forces that vary depending on the kind of polymer [3,4]: Due to their advantageous blend qualities, biomedical and pharmaceutical devices should utilize two polymers that can create hydrogen bonds when blended [1].

The PVA fiber has high tensile and shear strengths, tensile modulus, and wear resilience due to its maximal rigid lattice modulus. It is a synthetic polymer that comes in the form of a granular powder that is odorless. The PVA has attracted an increasing amount of interest in the biomedical area because to the fact that it is bio-inert. Many researchers have investigated the possibility of employing the PVA as a filler or in cross-linked products [5–7]. In addition to its many other applications, it has seen used extensively as a thermoplastic polymer for the production of non-toxic, harmless, and living tissues [3,8].

Polyacrylamide (PAAm) is a material that dissolves in water with a wide range of industrial flocculant applications. The PAAm and its derivatives have great attention in recent years due to their high molecular weight, their ability to dissolve in water without resembling a monomer, and their non-toxicity. Their copolymers with other hydrophilic monomers and their metallic salts are used in many applications, including mining, water treatment, and others [9].The PAAm may be dissolved in various Polymers like polyethylene glycol (PEG), polyvinyl alcohol (PVA), and carboxymethyl cellulose(CMC) [5,10,11].

Blends of polymer (PVA) with polymer (PAAm) have been determined through mechanical analysis in a variety of ways by many researchers: Gaurang Patel and Mundan B. Sureshkumar, two of the researchers, have conducted a study on the miscibility of PVA and PAAm in various proportions by employing the solution-cast technique.They have discovered that variations in FTIR, UV–Vis, TGA, SEM, and mechanical measurements indicated the interactions between the two polymers [12].El-din et al. studied the miscibility of PVA with PAAm in different proportions using the solution-cast method and gamma radiation up to 100 kGy. Visual inspection and reflectance tests demonstrated that the PVA/PAAm blends are miscible throughout a broad composition range [13].The X-ray diffraction examination confirmed the creation of a complex between the polymer mixture and the Ag NPs [14].

Electrospinning is a technique that is being utilized in the present study, and it is the way that is most often employed for the manufacturing of nanofibers [15,16] because of the ease its of use and capacity to work with several polymers .The electrospinning process is used to create fibers from a wide variety of polymers, both synthetic and natural, including biopolymers, with diameters ranging from tens of nanometers to a few micrometers [17,18]. In this study, two existing polymers were blended to create a new polymer, which was based on Poly(vinyl alcohol)/Poly (acrylamide) (PVA-PAAm) and compared among the prepared samples for optical and communication applications.

4. Experimental part

4.1. Materials

The particulate polymer PVA used was bought from Himedia, India, and had a high purity level of 99.0% and M_W=(85,000-126000) g/mol. Polymer PAAm was produced commercially by British Drug Houses (BDH) and had an extremely high purity level of 99.99% and M.W = $5*10^5$ g/mol.

4.2.Purification of PVA, PAAm, and PVA-PAAm nanofibers

A PVA of 1g was dissolved in 20 ml of purified water with constant agitation for 1.5h at a 50 ^oC. The solution PAAm was prepared by adding 1g to the blend and continuing to stir it for 2h at 50^0C, albeit in intermittent doses. The process was repeated many times until a sufficiently thick liquid resulted. To get a suitable polymer combination, a PVA-PAAm (50/50 wt.%) ratio was used. The procedure, which took

2h, requires constant mixing by swirling until the fluid become homogenous.

4.3.Electrospun

The ready-to-use mixtures were transferred into a 2 ml pipette using a metal capillary needle with an interior diameter of 0.5 mm. The electrospun procedure was performed in a temperature-controlled environment at a flow rate of 0.5 ml per hour using a hypodermic pump. The aluminium foil-covered cylinder that was used in the production of the electrospun nanofibers rotated at a rate of 1679 rotations per minute. The needle tip was positioned 10 cm away from the drum, and a voltage of 12 kV was applied.

.

4.4 Characterization of PVA-PAAm nanofibers after preparation.

This surface of electrospun nanofibers was analyzed using a FESEM. Patterns of XRD were taken using (λ =0.1542nm). The chemical composition of the nanofibers mats was investigated by FTIR spectroscopy at RT with a spectrometer (Thermo Nicolet, Nexus670, USA) that has a spectrum range of (4000-400)cm^{-1} and a UV-Visible Spectrophotometer(Shimadzu, UV-1800A) that measures light at a frequency of (200-1100)nm.

4.2 The Surface morphology and structural properties

4.2.1 Field Emission Scanning Electron Microscope (FE-SEM)

FE-SEM images at 35kx, 135kx, and 20kx, 50kx magnifications, respectively, show the surface morphologies of pure PVA and PAAm nanofibers as in Fig.1. Nanofibers electrospun from pure PVA and PAAm exhibit a consistent structure and a smooth surface, with no evidence of a bead on a string morphology. To the naked eye, nanofibers display a clean surface. Having the right concentration of polymer and solvent ensures a continuous, bead-free manufacturing process and eliminates the risk of switching to an electrostatic spraying method instead of electrospinning. Concernning electrospinning, the minimum concentration of PVA and PAAm needed changes with molecular weight [19]. Nanofibers made of PVA have an average diameter of 214.12nm, whereas those made of PAAm are 317.1nm on average.

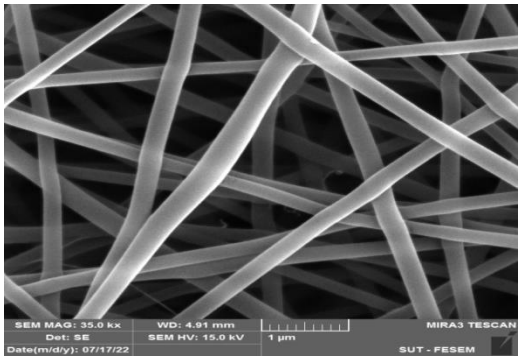

a

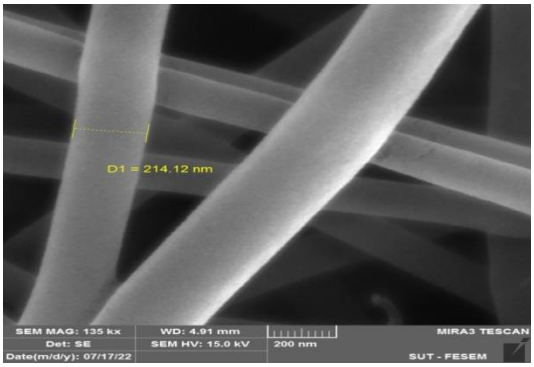

b

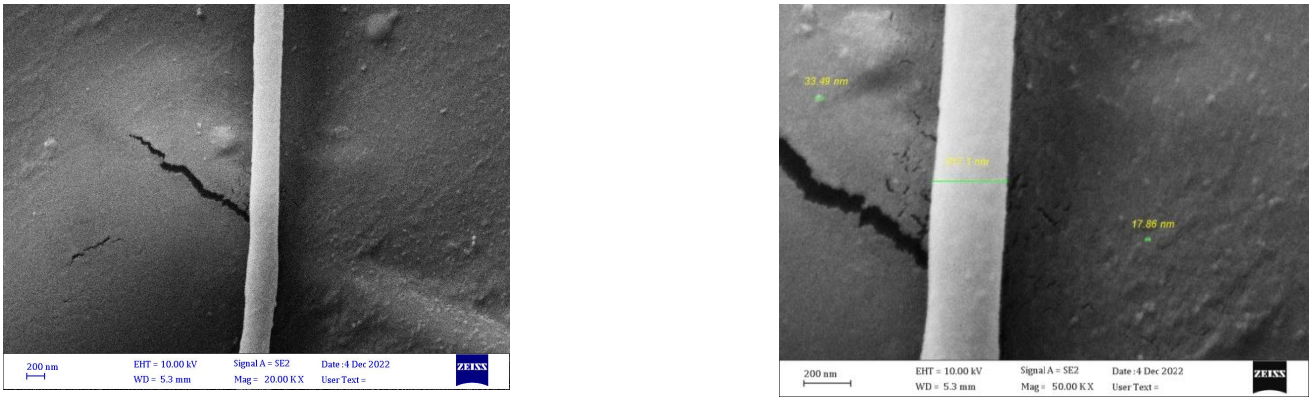

c **d**

Fig.1: Images obtained by (FE-SEM) at 35kx, 135kx, 20kx, and 50kx magnifications of electrospun PVA (a and b) and PAAm (c and d) nanofibers, respectively.

Images which were obtained with a scanning electron microscope at 35kx and 135kx magnifications of scanned PVA-PAAm electrospun nanofibers are shown in Fig. 2 .The PVA-PAAm solution can produce random strands of fibers, with an average diameter of 157.40 nm and a very smooth surface calculated using the software (Imge J). The experimental results and theoretical analysis depicted in the figures reveal that the viscosity of the solution has a significant impact on the diameter of the electrospun fibers, which may alter the form of the droplet, and can cause the jet to be unstable; However, we still face challenges in precisely controlling the diameter, morphology and porosity of electrospun fibers [19,20]. There is a direct correlation between the shear viscosity of the fluid and the average diameter of the electrospun nanofiber, denoted by d. Additionally, it has been established that bigger nanofiber sizes were produced when the typical viscosity of the fluid is high, according to the formula($d \sim \eta \lambda$) where λ stands for the scaling rule produce exponents larger than 1/3 the value of this exponent may vary with the type of polymer solution that is employed [19]. It is essential that the voltage and viscosity of the electrospun polymer fluid fall within a well-defined range; outside of this range, electrospinning cannot be accomplished. Polymer threads could be halted if the viscosity was too low (electrostatic spraying). Polymer is high viscosity (hardening at needle tip). Certain polymers have the lowest required viscosity. The polymer in the fluid to be electrospun is based on the molecular weight of the polymer and the type of solvent determines the concentration.

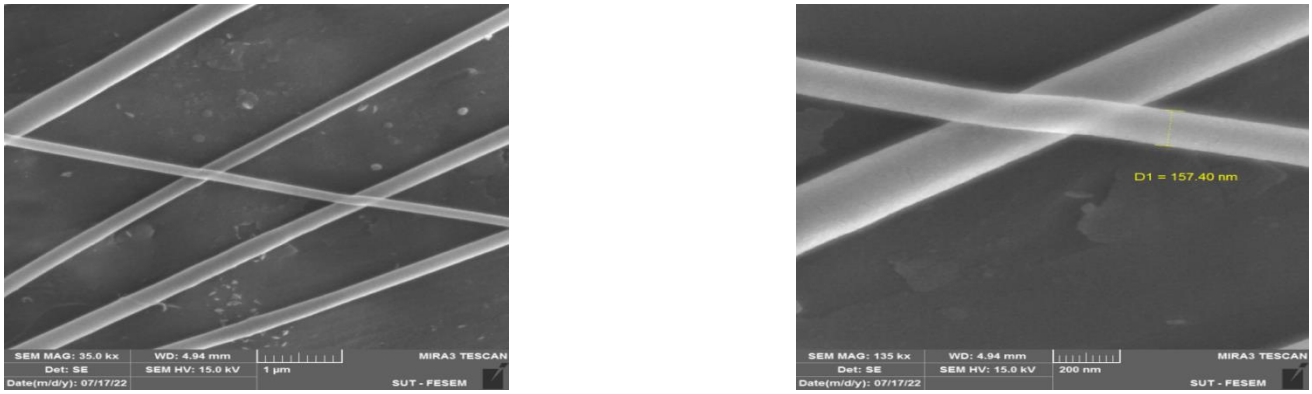

a **b**

Fig. 2. Images obtained by (FE-SEM) at 35kx and 135kx magnifications of electrospun PVA-PAAm nanofibers

4.2.2 X-ray diffraction analysis

X-ray diffraction patterns with a Cu Kα (=1.5406 A°) were employed to determine the structure of PVA, PAAm polymer nanofibers, and PVA-PAAm polymer blend at RT. The measurements of the diffractogram were carried out at 2θ ranging from 10° to 80. It is demonstrated here that PVA nanofibers had a semicrystalline nature, and the peak at 22.58° and the peak of PAAm at 21.05°and the nanofibers polymeric blend is shown a semicrystalline structure, the peak of which observed at 19.58° and it deviates to 23.21° which is by the plane (101) reflection see Fig.3, the pure nanofibers that agree very well with those found in the literature [14].

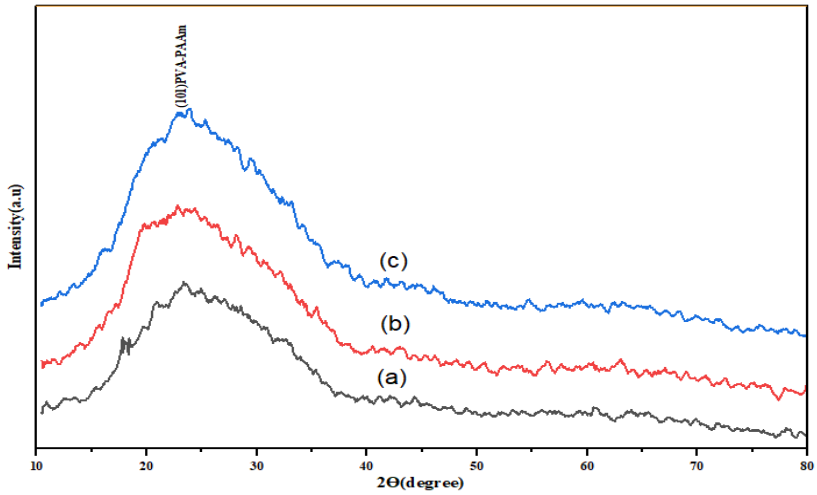

Fig. 3: The XRD of (a) PVA. (b) PAAm, and (c) PVA-PAAm blend.

4.2.3 Spectroscopy the Fourier transforms infrared (FTIR)

The ion peaks that are associated with the vibrational frequencies that occur between the links formed by the atoms that make up the substance serve as an important fingerprint in an infrared spectrum. Due to the unique composition of each material, no two substances will have the same IR range. Because of this, IR spectroscopy can be used to identify (qualitatively analyze) any kind of substance [21]. Fig. 4 shows the FTIR spectroscopy of the pure PVA, PAAm, and blend PVA-PAAm nanofibers. The spectrum that was recorded reveals distinctive bands that are caused by oscillations in the functional groups caused by elongation and twisting of the groupings of the produced film.

The characteristic peaks of PVA locate at 3423.20 cm^{-1}, 2895 cm^{-1}, 1730 cm^{-1}, and 1141 cm^{-1} in the spectrum of PVA [11]. Bands at 1730 cm^{-1} C=O stretching and 1141 cm^{-1} were attributed to C-O bending; a broad, very powerful band was observed at 3423.20 cm^{-1}, which was attributed to the O-H and N-H stretching vibration and indicated the presence of O-H hydroxyl groups in the pure PVA nanofibers [12]. The FTIR spectrum of PAAm exhibits a band at 3105 cm^{-1}, which has been assigned to symmetric and asymmetric stretching vibrations of N–H and O–H, bands at 2960 cm^{-1} have been assigned to symmetric and asymmetric stretching vibrations of C–H, bands at 1662.63 cm^{-1} C=O stretching and 1450.46 cm^{-1} have been assigned to C–H bending. Additionally, bands at 1328 cm^{-1} C–H bending and 1110.9 cm-1 C–O stretching [9]. Fig. 4 demonstrates the FTIR spectra of pure PVA and PAAm nanofibers and blend PVA-PAAm nanofibers. The vibrational bands at 3423.20cm^{-1} and 3105cm^{-1} assigned to O–H and N–H bending of pure PVA and PAAm nanofibers is shifted to 3473.79 cm^{-1} and 3414 cm^{-1}, the FTIR analysis of the PVA-PAAm hydrogel reveals that the PAAm and PVA networks are strongly hydrogen-bonded to one another at the N-H of PAAm chains and the O-H of PVA chains [11].

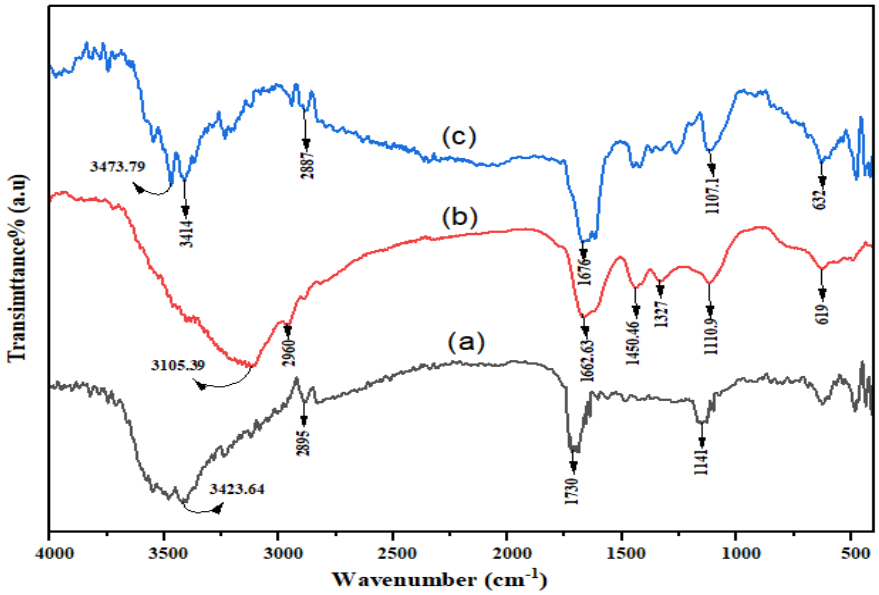

Fig. 4. FTIR spectra of (a) poly(vinyl alcohol) (PVA), (b) poly(acrylamide) (PAAm), and (c) PVA-PAAm blend.

5.3 Optical Properties

Fig.5 shows absorption patterns in the ultraviolet and visible ranges of the polymer pure PVA, PAAm, and PVA-PAAm blend. These spectra were obtained in the (200–1100) nm wavelength range at RT. These spectra were taken at RT and span from (200-1100) nm in wavelength. All of the coatings have strong UV absorbance and minimal Visual absorption, as is evident. The subsequent explains for this observation is as follows: Photons incident on a material at long wavelengths are not absorbed because they are insufficiently energetic to interact with atoms; photons incident on a material at lower wavelengths (near the basic absorption edge) interacting with the substance, which results in absorption. When a molecule consumes energy, a specific type of transition takes place in which the electron is boosted from an occupied orbit (σ, n or π) to a non-occupied

orbit (σ*or π*) with a high energy level. Transitions (n -π*) or (π-π*) create a peak in the UV-Vis band, indicating the presence of C=O and C=C of unsaturated bonds primarily of the polymer mix; the energy gap is largely determined by transitions (π-π*) transitions in particular [22–24]. The formula that was used to determine the absorption coefficient α(cm)$^{-1}$ is denoted by equation 1 [25].

$$\alpha = 2.303 \left(\frac{A}{t}\right) \quad (1)$$

The α(cm)$^{-1}$ vs hυ(eV) of the polymer pure PVA, PAAm, and PVA-PAAm blend are shown in Figure 6. It may be inferred by ion transformation is unlikely since ion absorption is excellent at high energies but rather poor at low energies. Absorption coefficients below 10^4 cm^{-1} suggest a high probability of indirect transfer [26]. It is possible to see the shift in the band gap energy by observing the absorption edge of the doped mixture; this shift is caused by the varying degree of the presence of semi-crystallinity within the polymer material. Energy band gaps for nanofiber films were calculated using the Tauc equation 2 [27].

$$(\alpha h\upsilon)^m = B\left(h\upsilon - E_g{}^{opt} \pm E_{ph}\right) \quad (2)$$

In both kinds (allowed and forbidden), the intercept of the extended linear component of the parabola was used to calculate the indirect optical energy gap for nanofiber sheets made of pure PVA, PAAm, and PVA-PAAm versus the photon energy $(h\upsilon)$ at $(\alpha h\upsilon)^m = 0$, as shown in Figs. 7 and 8, respectively. The goal was to measure the depth of the indirect optical energy gap. In Table1, we can see the optical band gap values for all of the samples, as shown in Table 1. Polymer nanofiber optical characteristics might be affected by a change in ion structure [28,29].

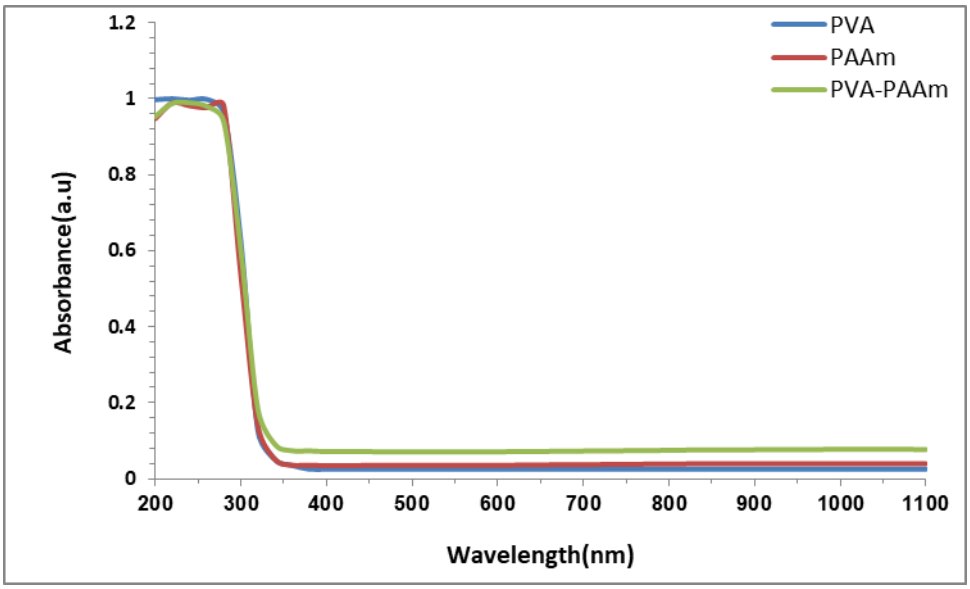

Fig. 5: The absorbance spectra of PVA, PAAm, and blend PVA-PAAm nanofibers.

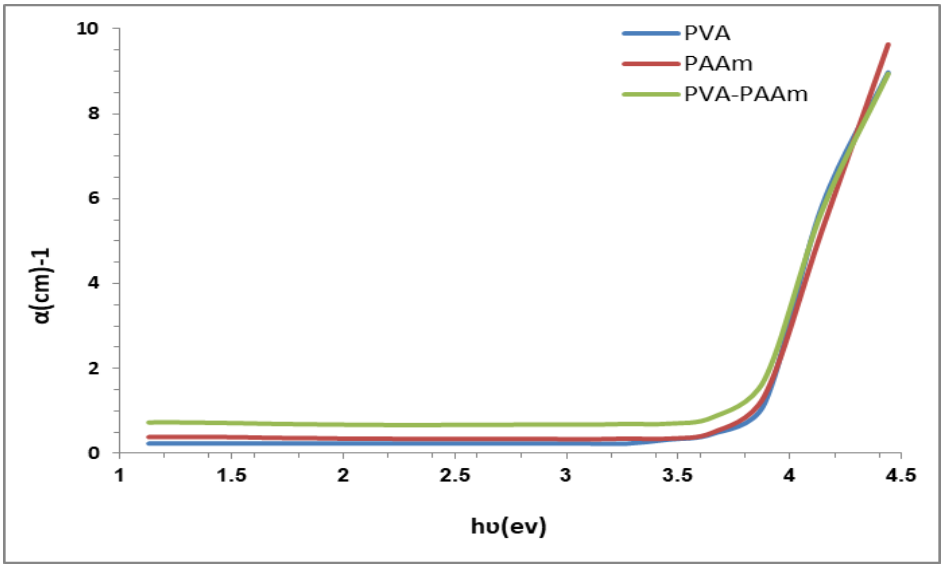

Fig. 6: Absorption coefficient spectra as a function of photon energy for PVA, PAAm, and blend PVA-PAAm nanofibers.

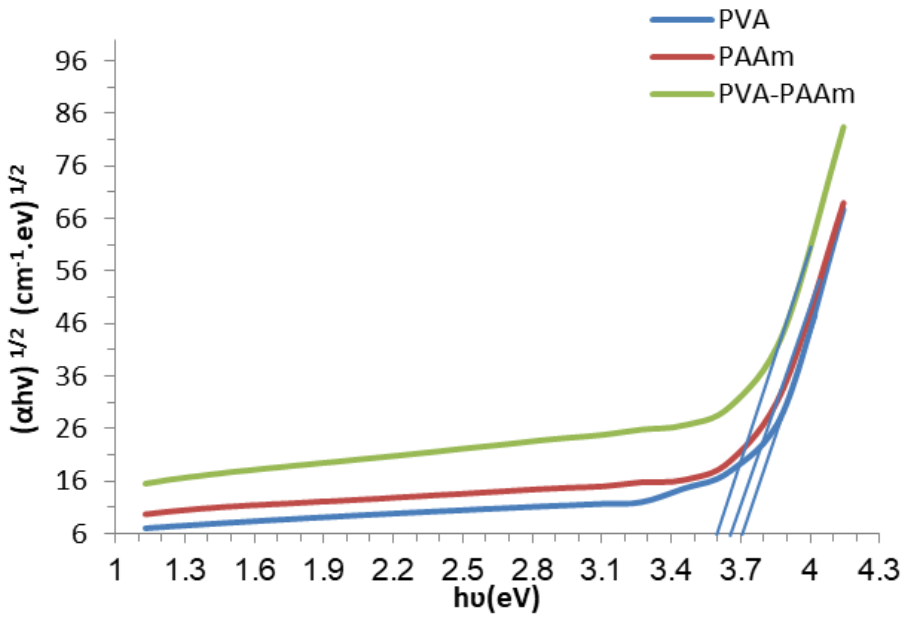

Fig. 7: A plot$(\alpha h\vartheta)^{\frac{1}{2}}$ versus photon energy $(hv)$of PVA, PAAm, and blend PVA-PAAm nanofibers.

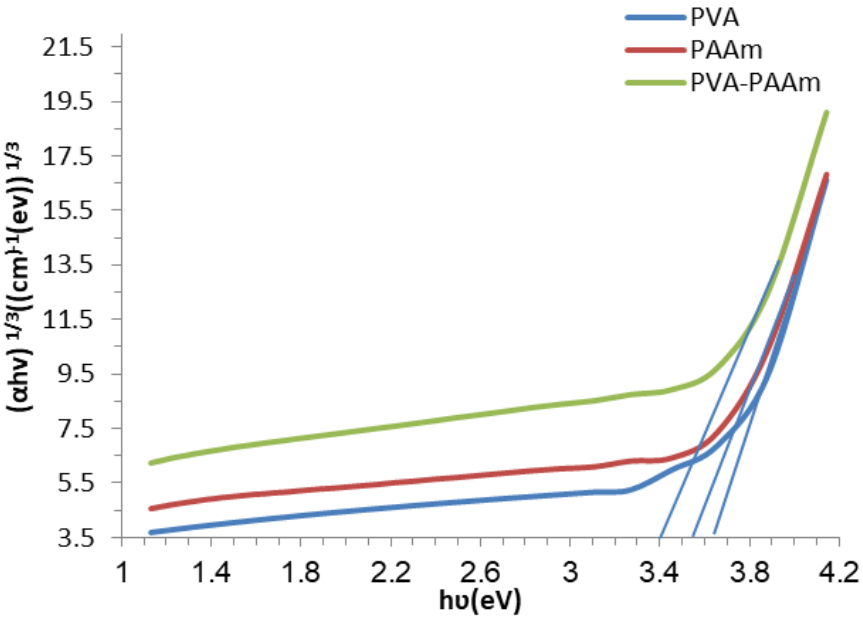

Fig. 8: A plot$(\alpha h\vartheta)^{\frac{1}{3}}$ versus photon energy $(h\nu)$ of PVA, PAAm, and blend PVA-PAAm nanofibers.

Table 1: Optical indirect energy gap (allowed and forbidden) for the prepared nanofibers.

Sample	$E_g^{in}eV(allowed)$	$E_g^{in}eV(forbidden)$
PVA	**3.70**	**3.65**
PAAm	**3.65**	**3.55**
PVA- PAAm	**3.60**	**3.40**

The formulas (3and 4) for determining the refractive index (n) and the extinction coefficient (k_o) are provided below [27]:

$$n = \frac{(R+1)}{(R-1)} + \left(\frac{4R}{(1-R)^2} - K_0^2\right)^{1/2} \quad (3)$$

$$k_o = \frac{\alpha\lambda}{4\pi} \quad (4)$$

Fig. 9 shows the wavelength-dependent refractive index (n) of PVA, PAAm, and PVA-PAAm nanofibers. It can be seen that as the PVA-PAAm increases the (n) increases.

This unusual behavior may be attributed to the increasing in the concentrations of nanofibers. Light with a high refractivity in the ultraviolet area will interact with a sample, increasing the (n) values of the sample. Fig.10 shows how the (K_o) of PVA, PAAm, and PVA-PAAm nanofibers vary with wavelength, optical absorption, and photon dispersion in the PVA-PAAm polymer blend increase. The increases in the PVA-PAAm polymer blend are accompanied by increases in the (K_0).This property may be associated with the high absorbance of nanofiber samples, which leads to a high (k_o) of nanofibers at UV wavelengths. Since the nanofiber $\alpha(cm)^{-1}$ is almost constant from the visible to the near-infrared spectrum, the nanofiber (K_o) likewise increases with increasing wavelength.

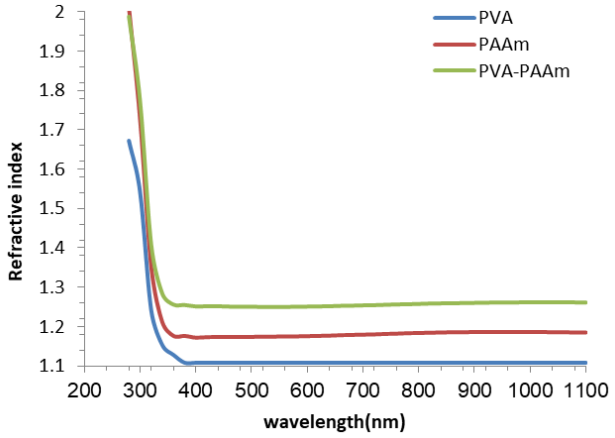

Fig. 9: The refractive index(n) of PVA, PAAm, and blend PVA-PAAm nanofibers.

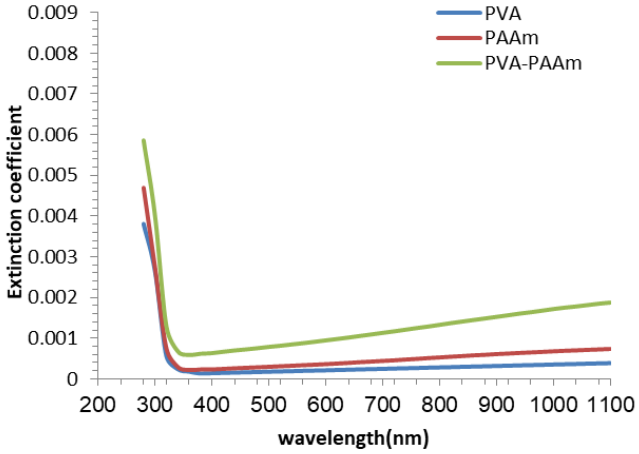

Fig. 10: The extinction coefficient (K_o) of PVA, PAAm, and PVA-PAAm blend nanofibers.

5.4 Dispersion Parameters

Dispersion parameters were examined and diagnosed using the Wemple DiDomenico model. The values of E_0, E_d, E_g, n_0, M_{-1} and M_{-3} were calculated using the formulas (5,6,7) [30]. Taken from a graphic showing the relationship between $(n^2-1)^{-1}$ and $(h\vartheta)^2$ in Fig.11, used the slope$(E_0\,E_d)^{-1}$ and the intercept$(\frac{E_0}{E_d})$ to determine E_0 and E_d. The Table (2) the energy gap band was calculated (the approximation relation $E_0 \approx 2E_g$) using the Tauc relation and the Wemple-DiDomenico estimate had similar values, the findings are consistent with previous studies [30].

$$(n^2-1)=\frac{E_d\,E_o}{{E_o}^2-(h\upsilon)^2} \quad (5)$$

$$E_o^2=\frac{M_{-1}}{M_{-3}} \quad (6)$$

$$E^2{}_d=\frac{M_{-1}^3}{M_{-3}} \quad (7)$$

The Urbach tail equation can be found using the relation given below [31].

$$\alpha=\alpha_0\exp(\frac{E}{E_U}) \quad (8)$$

Where E_U is Urbach energy (the approximation relation $E_U=\frac{1}{slope}$), and α_o is a constant. There was an increase in Urbach energy values at blend PVA-PAAm, which increased the

degree of amorphousness, as their values were tabulated in Table 2 along the slope of the relation shown in fig.12.

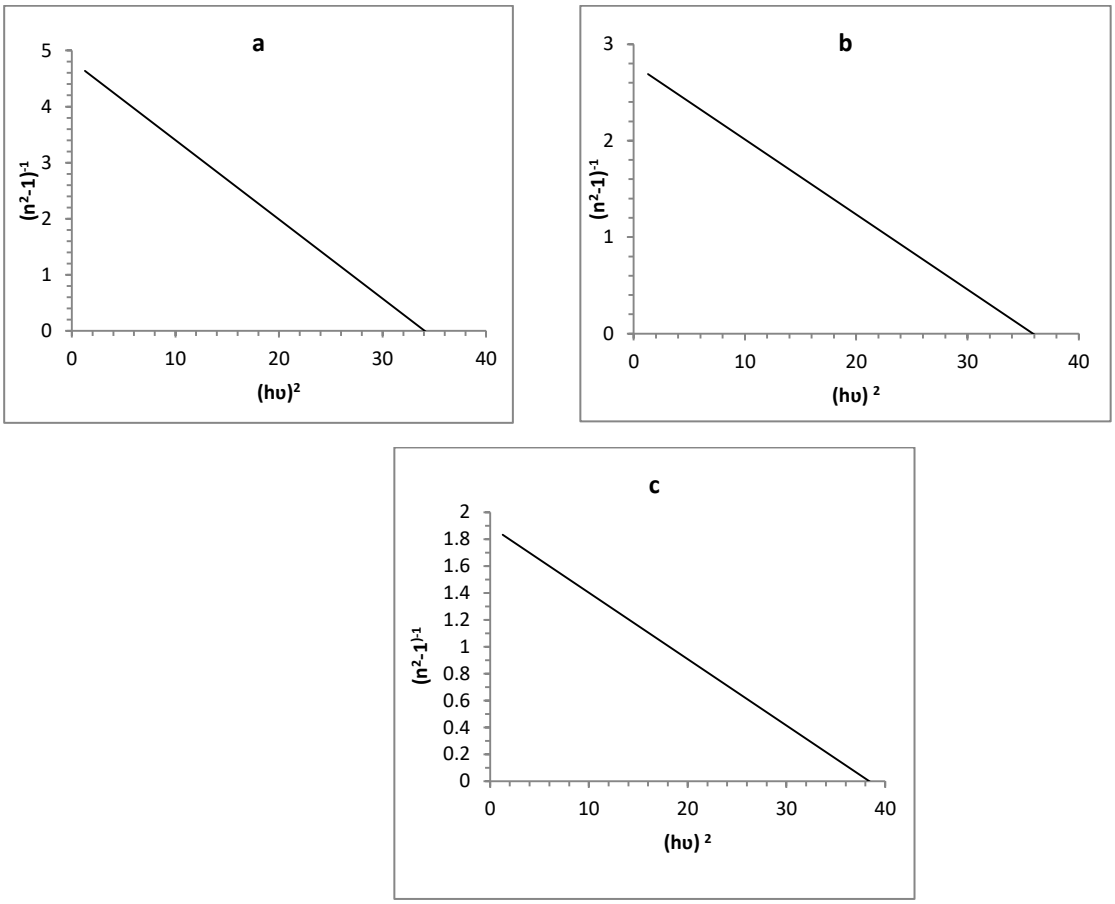

Fig.11: Plot of $(n^2 -1)^{-1}$ vs $(h\upsilon)^2$ of (a) PVA, (b) PMMa, and (c) blend PVA-PAAm nanofibers.

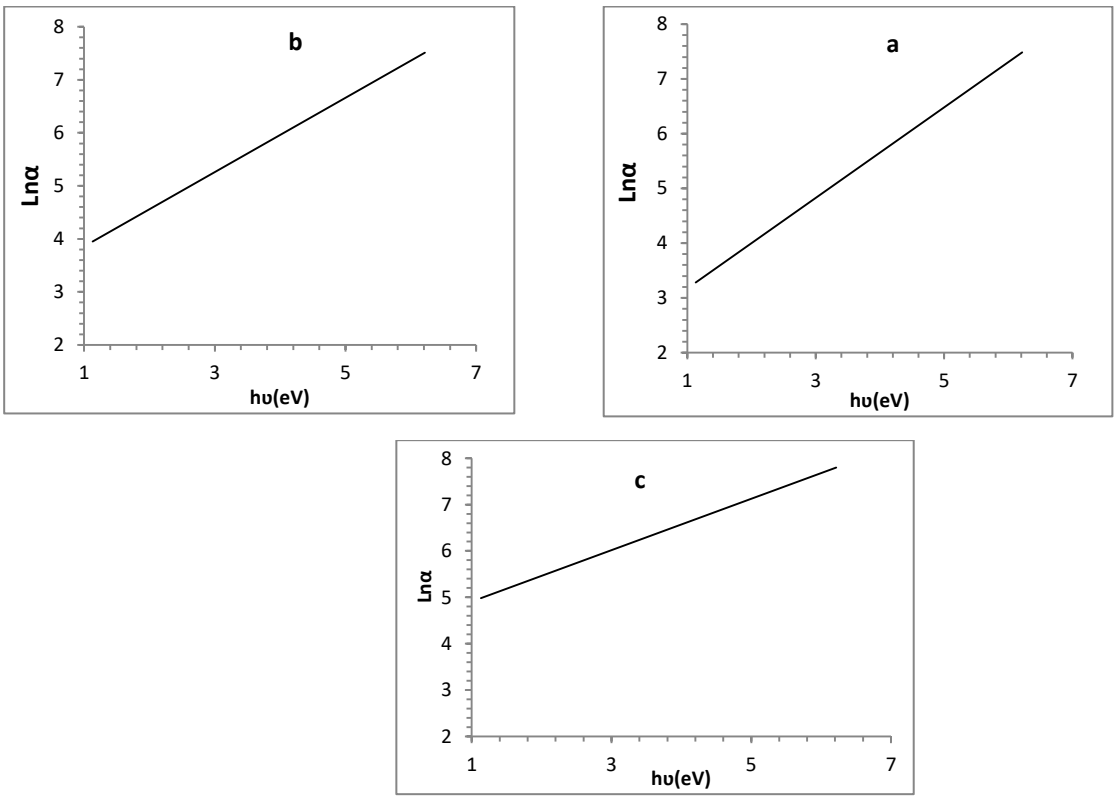

Fig.12: Plot of Lnα vs hυ(eV) of (a) PVA, (b) PMMa, and (c) blend PVA-PAAm nanofibers.

Table 2: Dispersion parameters of PVA, PAAm, and blend PVA-PAAm nanofibers.

parameter	PVA	PAAm	Blend PVA-PAAm
$E_0 eV$	7.0711	6.5580	7.0712
$E_d eV$	1.4141	2.1739	3.5360
$E_g eV$	3.5355	3.3032	3.5356
$n_0^2(0)$	1.1970	1.3314	1.5000
$n_0(0)$	1.1094	1.1538	1.2247
ε_∞	1.1970	1.3314	1.5000
M_{-1}	0.1818	0.3314	1.9997
$M_{-3} eV^{-2}$	0.0036	0.0077	0.03999
$E_U eV$	1.2094	1.4279	1.8044

6. Conclusion

Electrospinning the polymers PVA, PAAm, and blend PVA-PAAm samples yields a heterogeneous of fine fibers with average diameters (214.12,317.1 and 157.65) nm and a smooth surface, as shown by FESEM. XRD showed that the film polymeric of PVA, PAAm polymeric blend PVA-PAAm is displayed to have a semicrystalline nature. The FTIR observation indicates the PVA-PAAm networks are strongly hydrogen-bonded to one another of PAAm chains and PVA chains. According to the predicted optical energy gaps of indirect allowed and forbidden from the absorption spectra, the energy gap band decrease of blend (PVA-PAAm). The calculated energy gap by Wemple-DiDomenico was compatible with the value of the optical energy gap calculated by the Tauc relation and Urbach energy values increased.

References

[1]M.Z. Esfahani, B. Baghaei, M. Arabian, M. Keivani, M. Salehi, Polypropylene nanofibre, 2011.

[2]R.M. Radwan, Electron induced modifications in the optical properties of polypropylene, J. Phys. D. Appl. Phys. 40 (2007) 374–379. https://doi.org/10.1088/0022-3727/40/2/014.

[3]W. Klonowski, Introduction to polymer physics, 1997. https://doi.org/10.1016/s0097-8485(97)00027-2.

[4]Al-Jamal, A.N., Hadi, Q.M., Hamood, F.J., Abass, K.H., "Particle size effect of Sn on structure and optical properties of PVA-PEG blend", Proceedings - International Conference on Developments in eSystems Engineering, DeSE, pp. 736-740, 2019. DOI: 10.1109/DeSE.2019.00137

[5]Z. Yang, H. Peng, W. Wang, T. Liu, Crystallization behavior of poly(ε-caprolactone)/layered double hydroxide nanocomposites, J. Appl.

Polym. Sci. 116 (2010) 2658–2667. https://doi.org/10.1002/app.

[6]C.H. Cholakis, W. Zingg, Effect of heparin–pva hydrogel on platelets in a chronic canine arterio-venous shunt - Cholakis - 2004 - Journal of Biomedical Materials Research - Wiley Online Library, J. Biomed. …. 23 (1989) 417–441. http://onlinelibrary.wiley.com/doi/10.1002/jbm.820230404/abstract%5Cnpapers2://publication/uuid/8A73B62F-E67F-4517-BC8E-DB897C5F95F0.

[7] S. Horiike, S. Matsuzawa, Application of syndiotacticity-rich PVA hydrogels to drug delivery system, J. Appl. Polym. Sci. 58 (1995) 1335–1340. https://doi.org/10.1002/app.1995.070580815.

[8]W.K. Kadhim, M.K. Alshmmari, M.A. Al-ethary, Synthesis and Characteristics of (PAV-PAVC-Ti) Nanocomposites, 1 (2020) 23–30.

[9]G. Herth, G. Schornick, F. L. Buchholz, Polyacrylamides and Poly(Acrylic Acids), Ullmann's Encycl. Ind. Chem. (2015) 1–16. https://doi.org/10.1002/14356007.a21_143.pub2.

[10] H. Zhang, D. Zhai, Y. He, Graphene oxide/polyacrylamide/carboxymethyl cellulose sodium nanocomposite hydrogel with enhanced mechanical strength: Preparation, characterization and the swelling behavior, RSC Adv. 4 (2014) 44600–44609. https://doi.org/10.1039/c4ra07576e.

[11] K. Ou, X. Dong, C. Qin, X. Ji, J. He, Properties and toughening mechanisms of PVA/PAM double-network hydrogels prepared by freeze-thawing and anneal-swelling, Mater. Sci. Eng. C. 77 (2017) 1017–1026. https://doi.org/10.1016/j.msec.2017.03.287.

[12] G. Patel, M.B. Sureshkumar, Preparation of PAM/PVA blending films by solution-cast technique and its characterization: A spectroscopic study, Iran. Polym. J. (English Ed. 23 (2014) 153–162. https://doi.org/10.1007/s13726-013-0211-x.

[13] H.M.N. El-din, A.W.M. El-Naggar, F.I. Ali, Miscibility of poly(vinyl alcohol)/polyacrylamide blends before and after gamma irradiation, Polym. Int. 52 (2003) 225–234. https://doi.org/10.1002/pi.1003.

[14] H.M. Ragab, A. Rajeh, Structural, thermal, optical and conductive properties of PAM/PVA polymer composite doped with Ag nanoparticles for electrochemical application, J. Mater. Sci. Mater. Electron. 31 (2020) 16780–16792. https://doi.org/10.1007/s10854-020-04233-6.

[15] M. Al Shafouri, N.M. Ahmed, Z. Hassan, M.A. Almessiere, Structural and Optical Properties of Nanofibers Prepared with Electrospinning by Using PMMA Integrated with Curcuminoids to Produce White LED, 21 (2020) 1733–1742. https://doi.org/10.1007/s12221-020-9783-1.

[16] N.Z. Al-hazeem, N.M. Ahmed, M.Z.M. Jafri, A. Ramizy, The effect of deposition angle on

morphology and diameter of electrospun TiO_2/PVP nanofibers, Nanocomposites. 7 (2021) 70–78. https://doi.org/10.1080/20550324.2021.1917836.

[17] G. Rüzgar, M. Bİrer, S. Tort, F. Acartürk, Studies on Improvement of Water-Solubility of Curcumin With Electrospun Nanofibers, 90 (2016) 143–149.

[18] Y. Lu, K.W. Shah, J. Xu, Synthesis , Morphologies and Building Applications of Nanostructured Polymers, (2017). https://doi.org/10.3390/polym9100506.

[19] D.W. Schubert, Revealing novel power laws and quantization in electrospinning considering jet splitting—toward predicting fiber diameter and its distribution, Macromol. Theory Simulations. 28 (2019) 1900006.

[20] Q. Wang, S. Liu, L. Fu, Z. Cao, W. Ye, H. Li, P. Guo, X.S. Zhao, Electrospun γ-Fe2O3 nanofibers as bioelectrochemical sensors for simultaneous determination of small biomolecules, Anal. Chim. Acta. 1026 (2018) 125–132. https://doi.org/10.1016/j.aca.2018.04.010.

[21] P. Jayaprakash, S. Suriya, D.G. Prakash, P.B. Bhargav, Vibrational Spectroscopic and Optical Absorption Studies on PVA based Polymer electrolytes, 584 (2012) 546–550. https://doi.org/10.4028/www.scientific.net/AMR.584.546.

[22] A. Satrijo, Controlling the Architectures and Optical Properties of Conjugated Polymer Aggregates and Films by, (2007).

[23] G.O. Synthesis, Supplementary information Tuning the Bandgap and Absorption Behaviour of the Newly-Fabricated UHMWPEO-PVA / GO Hybrid Nanocomposites Transmittence / %, 70 (2021) 6140.

[24] R.A. Ghazi, K.H. Al-Mayalee, E. Al-Bermany, F.S. Hashim, A.K.J. Albermany, Impact of polymer molecular weights and graphene nanosheets on fabricated PVA-PEG/GO nanocomposites: Morphology, sorption behavior and shielding application, AIMS Mater. Sci. 9 (2022) 584–603.

[25] Ingham JD, Lawson DD (1965) Refractive index-molecular weight helatlonships. J Polym Sci A 3: 2707–2710. https://doi.org/10.1002/pol.1965.100030728.

[26] A.I. Abdelamir, E. Al-bermany, F.S. Hashim, Enhance the Optical Properties of the Synthesis PEG / Graphene- Based Nanocomposite films using GO nanosheets Enhance the Optical Properties of the Synthesis PEG / Graphene- Based Nanocomposite films using GO nanosheets, (2019). https://doi.org/10.1088/1742-6596/1294/2/022029.

[27] Haneen Abass, K., Haidar Obaid, N., "0.006wt.%Ag-Doped Sb_2O_3 Nanofilms with Various Thickness: Morphological and optical properties", Journal of Physics: Conference Series, 1294(2), 2019. doi:10.1088/1742-6596/1294/2/022005

[28] N. Rajeswari, S. Selvasekarapandian, S. Karthikeyan, C. Sanjeeviraja, International Journal of Polymeric Materials and Polymeric Biomaterials Lithium Ion Conducting Polymer Electrolyte Based on Poly (Vinyl Alcohol) – Poly (Vinyl Pyrrolidone) Blend with, (2012) 37–41. https://doi.org/10.1080/00914037.2011.641693.

[29] T. Hasan, B.J. Senger, C. Ryan, M. Culp, R. Gonzalez-rodriguez, J.L. Coffer, A. V Naumov, Optical Band Gap Alteration of Graphene Oxide via Ozone Treatment, Sci. Rep. (2017) 1–8. https://doi.org/10.1038/s41598-017-06107-0.

[30] S.H. Wemple, M. DiDomenico, Behavior of the electronic dielectric constant in covalent and ionic materials, Phys. Rev. B. 3 (1971) 1338–1351. https://doi.org/10.1103/Phys. Rev B.3.1338.

[31] F. Urbach, The long-wavelength edge of photographic sensitivity and of the electronic Absorption of Solids ,Phys. Rev. 92 (1953) 1324. https://doi.org/10.1103/Phys Rev.92.1324.